Check for updates

EXTENDED ABSTRACT

EUROSTRUCT

Analysis of the Joint Effects of Thermal Stresses and Corrosion on Integral Abutment Bridges

Alessandro Contento[1] | Angelo Aloisio[2] | Junqing Xue[1] | Giuseppe Quaranta[3] | Bruno Briseghella[1] | Paolo Gardoni[4]

Correspondence

Dr. Alessandro Contento
Fuzhou University
College of Civil Engineering
350108 Fuzhou, China
Email: alessandro@fzu.edu.cn

[1] Fuzhou University, Fuzhou, China
[2] University of L'Aquila, L'Aquila, Italy
[3] Sapienza University of Rome, Rome, Italy
[4] University of Illiois at Urbana-Champaign, Urbana, USA

Abstract

The corrosion of reinforced concrete structures in coastal areas turns out to be very severe and can extend significantly in windy zones. Additionally, frequent temperature changes and, above all, exposure to extreme temperatures might induce wider cracks and micro-cracks in concrete structures which, in turn, might accelerate the diffusion of corrosive agents. Motivated by this evidence, the present study aims at verifying the sensitivity of integral abutment bridges to the combined effect of thermal stresses and corrosion. Preliminary results show that a high thermal stress may amplify the negative effects of corrosion but also that the bridge used for the case study is more sensitive to thermal stresses than to corrosion.

Keywords

Corrosion, Thermal loads, Post-tensioned bridge, Serviceability limit state

1 Introduction

The corrosion of reinforced concrete structures highly depends on local environmental exposure conditions. For reinforced concrete structures in coastal areas, such deterioration phenomenon turns out to be very severe and can extend significantly in windy zones, since higher wind speeds allow the deposition of a larger concentration of chlorides further inland. And the larger concentration of chlorides, the larger the steel corrosion rate. The connection between chloride deposition rate and steel corrosion rate has been proved in several studies [1]. Additionally, frequent temperature changes and, above all, exposure to extreme temperatures might induce wider cracks and micro-cracks in concrete structures which, in turn, might accelerate the diffusion of corrosive agents. In the case of integral abutment bridges [2], even before compromising structural safety, the combination of corrosion and extreme temperature variations may lead to the exceedance of some serviceability limit states and to cascading negative effects on the proper operation of the road infrastructure.

Motivated by this evidence, the present study aims at verifying the sensitivity of integral abutment bridges to the combined effect of thermal stresses and corrosion. The final goal is to quantify the risk of exceedance of relevant serviceability limit states. For this purpose, the model of an existing bridge is used as a case study. Preliminary results show that high thermal stress may largely amplify the negative effects of corrosion and can anticipate the

exceedance of the considered serviceability limit states.

2 Modeling framework

To analyze the combined effects of thermal stresses and corrosion, an existing integral abutment bridge located in Shenzhen (Guangdong, China) is selected as a case study. In the analyses, the location of the bridge is changed from the real one, assuming that the bridge is positioned in parallel with a hypothetical shore at a distance variable between 10m and 100m. In addition to thermal loads and corrosion effects, the bridge is considered subject to traffic load.

This analysis considers three different limit states related to the maximum vertical displacement of the girders, the stresses in the lowest fiber of the concrete cross-section, and the stresses in the post-tensioned tendons.

2.1 Bridge model

The structural model of the Maluanshan bridge, which is an integral abutment bridge, is used in the analyses. Such a bridge is a three-span, post-tensioned bridge with a total length of 88 meters. Figure 1 shows a lateral view of the Maluanshan Bridge and a typical cross-section.

Since the purpose of the study is to verify the exceedance of the serviceability limit state, it is reasonable to assume a linear behavior of the bridge deck within the range of the

considered loads. Therefore, the structural components of the bridge are modeled with equivalent linear elements, one for each row of piers and six for each girder. The difference in the accuracy of the models of piers and girders is a consequence of the choice to analyze the effects of the chosen loads only on the girders. Each girder is divided into six elements to account for the changes in the section and position of the post-tensioned tendons. The elements used to model the girders are homogenized elements that account for the presence of both regular and post-tensioned steel. The interaction between abutments and back-fill is modeled with springs having a stiffness taken from the literature.
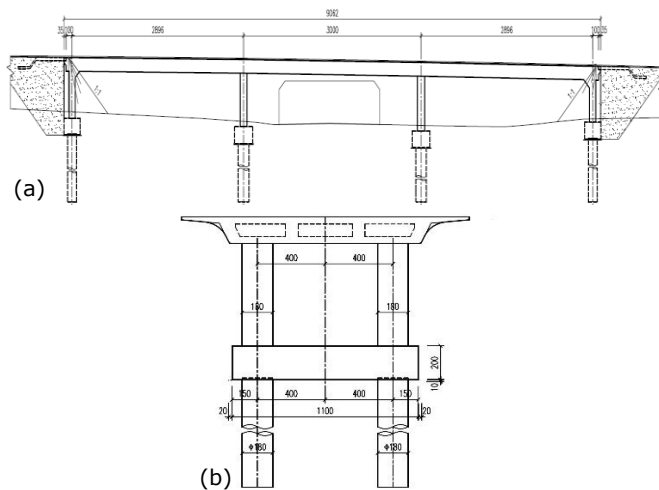

Figure 1 View of the Maluanshan integral abutment bridge in Shenzhen (a) and typical cross-section (b).

For the post-tensioned tendons, the long-term losses due to concrete shrinkage, concrete creep, and steel relaxation are modeled according to the formulation provided in Eurocode 2 [3]. The elastic problem is solved with the classical displacement formulation.

2.2 Temperature model

The thermal loads acting on the girders consist of uniform and linear gradients of temperature (ΔT_u and ΔT_l, both expressed in [°C]) that are assigned to each element of the girder. Such gradients are assumed to be the same for all the girders. Their values are based on temperature measurements referred to bridges in China, mostly in the Guangdong province. Such measurements refer to both winter and summer months which are the months expected to be characterized by the largest temperature variations.

A model for such gradients as functions of the environmental conditions at the site is currently been developed based on temperature measurements referred to similar bridges located in several provinces in China.

2.3 Corrosion model

Corrosion is modeled starting from the surface chloride concentration C_s according to the formulation presented by Yang et al. [4], which reads as

$$C_s = 0.64 A_c e^{-0.01d} v_w^{0.61}(1-e^{-1.25t})R_{W/B}. \tag{1}$$

In Equation (1), A_c is the correction coefficient for the binder type [4], d represents the distance from the coast [m], and v_w is the wind speed [m/s]. The time t is the exposure time in years and $R_{W/B}$ is the water-to-binder ratio. Since no wind speed data are available for the case study, Equation (1) is calibrated so that

$$C_s(d=10,t=\infty)=\mu_C, \tag{2}$$

where μ_C is the mean value of the distribution of C_s used in [5]. While for regular steel the value of C_s varies according to the distance from the shore (accounting also for the position of every single bar within the girders), for the post-tensioned tendons the distance is fixed to 15mm as in [6]. Starting from C_s, the time-dependent chloride diffusion within the concrete $C=C(s,t)$, which takes into account the time-dependent behavior of both surface chloride concentration C_s and chloride diffusion coefficient D, can be obtained following [7]; s represents the distance from the surface of the girder (i.e., the concrete cover). For the post-tensioned tendons, the time-dependent chloride diffusion also accounts for the chlorides in the grout that are assumed to have a concentration of 500ppm, following [6]. Once the time-dependent chloride diffusion within concrete is known, the corrosion current density i_{corr} [µA/cm2] is estimated following [8] as

$$\ln(1.08 i_{corr}) = 17.89 + 0.7771\ln(1.69C)$$
$$- 3006/T - 0.000116R_c + 2.24t^{-0.215}. \tag{3}$$

In Equation (3), T is the temperature in [K], and R_c is the ohmic resistance of concrete, which decreases as the chlorides increase [9]. The current intensity is used to derive both generalized and pit corrosion using the formulation provided in [10]. The location of the pit corrosion is assigned along each bar (and each strand in the tendons) with a continuous Poisson Process that can account for an increased probability of having pits near the location of the rebars.

2.4 Traffic load model

The traffic load is modeled according to the Chinese standard for bridges [11] which considers four design lanes for a transversal dimension of the deck of 17m, as in the bridge chosen for the case study. According to such a design code, the traffic load is assigned as the composition of a uniform load q_k and a concentrated load P_k, as in Figure 2.
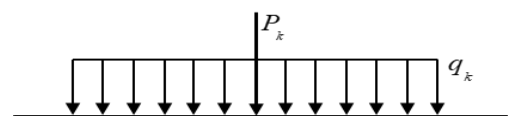

Figure 2 Scheme of the traffic load

The uniform lane load is distributed along the entire length of the bridge with the same sign, whereas the concentrated load is moved according to discrete steps of 0.1m which are the same steps used to verify stresses and

strains in the cross-sections of the girders.

3 Preliminary results

The analysis considers different scenarios obtained by combining the extreme values of the distributions of the temperature gradients (i.e., $\Delta T_u = \{-10°, 10°\}$ and $\Delta T_l = \{-5°, 5°\}$), the traffic load, and corrosion phenomena lasting 100 years. The results show that the bridge, as designed, has limited sensitivity to corrosion. These results can be partially explained by considering the limited amount of chlorides inside the post-tensioned tendons and, to a lesser extent, the large thickness of the concrete cover, which goes from 6cm for the steel bars near the upper and lower sides of the cross-section to 4cm for the steel bars on the lateral positions.

Figure 3 shows the maximum values of the vertical displacements v, obtained considering the different load combinations, along the length of the bridge (defined by an abscissa x [m]). From Figure 4, which is a zoom of Figure 3 in a limited range around the area of the largest displacements, it is possible to see that the largest displacement is close to 3mm and that, in any case, it is significantly lower than $v_{sl} = 0.048$m, which is the threshold imposed for the serviceability limit state by the Chinese standards [11].
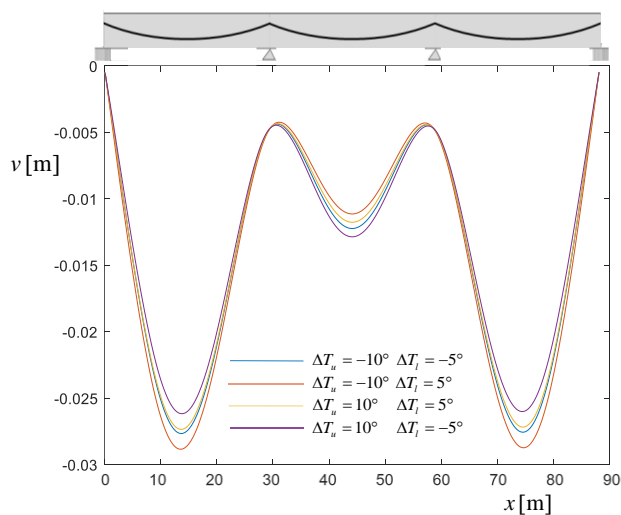

Figure 3 Bridge displacements for several combinations of the uniform and linear temperature gradients

Although the displacements are limited, when a large negative value of the uniform gradient of temperature is considered, the concrete stress at the bottom fiber of the cross-section σ_{ci} reaches the modulus of rupture strength $f_r = 4.2 \cdot 10^6$ N/m^2 (as shown in Figure 5), with the consequent occurrence of cracks. To account for the cracked sections, an effective moment of inertia I_e is used as an average value along the span of each element of the beam where $\sigma_{ci} > f_r$ according to the method proposed by Branson [12].
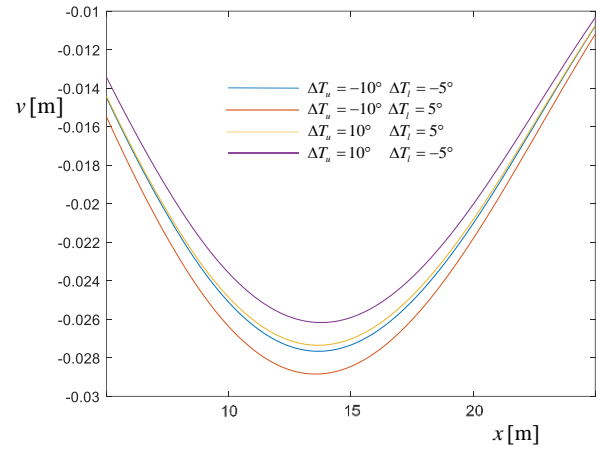

Figure 4 Zoom of Figure 3 in the range of the maximum displacements
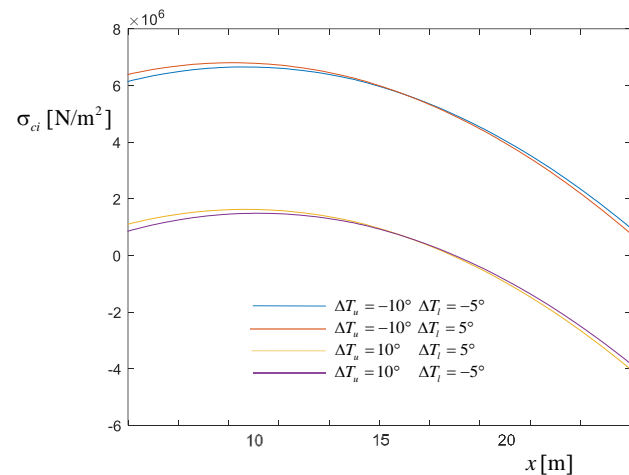

Figure 5 Concrete stresses at the bottom fiber of the cross-section

When the cracked sections are considered, as for the results in Figure 6, the displacements increase. For the worst combination of thermal gradients (i.e., ΔT_u =-10° and ΔT_l =5°), the largest displacement becomes larger than v_{sl} (i.e., v =0.05m), thus exceeding the serviceability limit state.
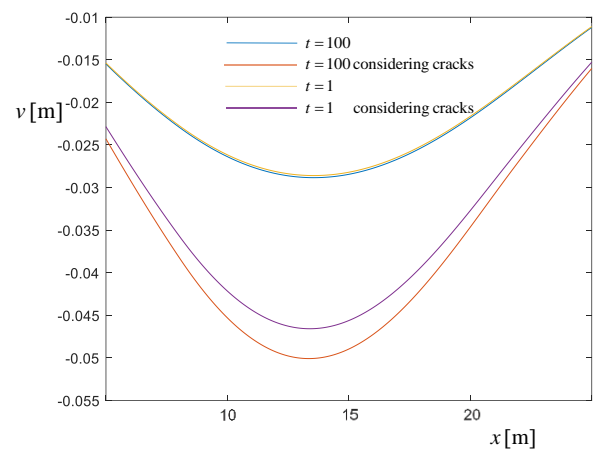

Figure 6 Comparisons between displacements at 1 and 100 years, with and without considering cracks

4 Conclusions

The results of the preliminary analyses show that there are cases where, in the long term, the combined effects of thermal loads, traffic load, and corrosion lead to displacements that exceed the threshold set for the serviceability limit state by the Chinese standards. Consequently, there is a need to accurately estimate the probability of loss of functionality of the bridges to help the design of actions needed to prevent such loss of functionality and the consequent impact on road infrastructure.

References

[1] Corvo, F.; Minotas, J.; Delgado, J.; Arroyave, C. (2005). *Changes in atmospheric corrosion rate caused by chloride ions depending on rain regime*. Corrosion Science 47 (4), pp. 883–892.

[2] Arockiasamy, M.; Butrieng, N.; Sivakumar, M. (2004). *State-of-the-art of integral abutment bridges: Design and practice.* Journal of Bridge Engineering 9 (5), pp. 497–506.

[3] EN 1992-1-2, 2004. Eurocode 2: *Design of Concrete Structures - Part 1-2*. 1st ed. Brussels: BSi.

[4] Yang, L.F.; Cai, R; Yu, B. (2017). *Investigation of computational model for surface chloride concentration of concrete in marine atmosphere zone*. Ocean Engineering 138, pp. 105–111.

[5] Papakonstantinou, K.G.; Shinozuka, M. (2013). *Probabilistic model for steel corrosion in reinforced concrete structures of large dimensions considering crack effects*. Engineering Structures 57, pp. 306–326.

[6] Nguyen, V.-S.; Jeong, M.C.; Han, T.S.; Kong, J.S. (2013). *Reliability-based optimization design of post-tensioned concrete box girder bridges considering pitting corrosion attack*. Structure and Infrastructure Engineering 9(1), pp. 78–96.

[7] Yang, L.F.; Ma, Q.; Yu, B. (2018). *Analytical solution and experimental validation for dual time-dependent chloride diffusion in concrete*. Construction and Building Materials 161, pp. 676-686.

[8] Liu, T.; Weyers, R.W. (1998). *Modeling the dynamic corrosion process in chloride contaminated concrete structures*. Cement and Concrete Research 28(3), pp. 365–379.

[9] Liu, Y. (1996). *Modeling the time-to-corrosion cracking of the cover concrete in chloride contaminated reinforced concrete structures*. PhD thesis, Virginia Tech.

[10] Val, D.V.; Melchers, R.E. (1997). *Reliability of deteriorating RC slab bridges*. Journal of Structural Engineering 123(12), pp. 1638–1644.

[11] JTG D60-2015, 2015. *General Specifications for Design of Highway Bridges and Culverts*. China Communications Press.

[12] Branson, D.E. (1977). *Deformation of concrete structures.* McGraw Hill, New York.